Virology 611 (2025) 110659

Contents lists available at ScienceDirect

Virology

journal homepage: www.elsevier.com/locate/virology

Brief Communication

A rapid and robust luciferase-based reporter system to assess SARS-CoV-2 protease activity

Alessandro Lucini Paioni [a,1,3], Lorena Donnici [a,1], Riccardo Nodari [a,b], Marika Longo Minnolo [a,b], Anastasia Ferraro [c], Alessia Alberico [c], Margherita Brindisi [c], Ernesto Mejías Pérez [d,e,f,g], Oliver T. Keppler [g,h], Vincenzo Summa [c], Luca G. Guidotti [i,j], Manuel Albanese [a,g,k,*,2], Raffaele De Francesco [a,b,2,**]

[a] Istituto Nazionale Genetica Molecolare "Romeo ed Enrica Invernizzi", Milan, Italy
[b] Department of Pharmacological and Biomolecular Sciences (DiSFeB), University of Milan, Milan, Italy
[c] Department of Pharmacy (DoE 2023-2027), University of Naples Federico II, Italy
[d] Departamento de Biología Celular, Fisiología e Inmunología, Universidad de Córdoba, Spain
[e] Instituto Maimónides de Investigación Biomédica de Córdoba (IMIBIC), Spain
[f] Hospital Universitario Reina Sofía, Córdoba, Spain
[g] Max von Pettenkofer Institute and Gene Center, Virology, National Reference Center for Retroviruses, Faculty of Medicine, LMU Muenchen, Munich, Germany
[h] German Centre for Infection Research (DZIF), Partner Site Munich, Munich, Germany
[i] Division of Immunology, Transplantation, and Infectious Diseases, IRCCS San Raffaele Scientific Institute, 20132, Milan, Italy
[j] Vita-Salute San Raffaele University, 20132, Milan, Italy
[k] Department for Clinical Sciences and Community Health (DISCCO) (DoE 2023-2027), University of Milan, Milan, Italy

ARTICLE INFO

Keywords:
SARS-CoV-2 reporter
Antiviral drugs
Protease inhibitors
SARS-CoV-2
Main protease (Mpro/3CLpro)

ABSTRACT

Despite effective antiviral drugs that have emerged to combat SARS-CoV-2 infections, novel therapeutic strategies are required to better address the ongoing and future evolutions of the virus. Targeting viral proteases, such as the main protease (Mpro), remains a promising approach. Here, we present a rapid and sensitive luminescence-based reporter system, the i-NSP4/5-Gluc2, to assess Mpro activity. This system employs Gaussia luciferase (Gluc) fused to a pro-interleukin 1β (pro-IL-1β) fragment containing a specific Mpro cleavage site. Upon Mpro cleavage, Gluc is released and secreted, generating a luminescent signal outside the cells. By optimizing the system's design and experimental conditions, we achieved high sensitivity and specificity. The i-NSP4/5-Gluc2 system was validated using the Mpro inhibitor Nirmatrelvir and successfully identified potential Mpro inhibitors from a small library of 46 compounds, as proof of concept. Notably, 13 out of 14 new compounds identified by the i-NSP4/5-Gluc2 assay exhibited potent antiviral activity against live SARS-CoV-2, highlighting the system's accuracy and predictive power. This BSL2-compatible, high-throughput approach facilitates rapid and efficient screening of antiviral compounds, accelerating the development of effective therapeutics against SARS-CoV-2 and future viral pandemics.

1. Introduction

The COVID-19 pandemic triggered a global research effort that led to the development of highly effective vaccines and antivirals in record time. These interventions have significantly reduced the severity of illness and mortality associated with the virus, helping to control the pandemic (Patel et al., 2022). To date, Severe Acute Respiratory Syndrome Coronavirus 2 (SARS-CoV-2) has been responsible for more than 700 million confirmed cases and more than seven million deaths (according to World Health Organization monitoring). However, the rapid

* Corresponding author. Istituto Nazionale Genetica Molecolare "Romeo ed Enrica Invernizzi", 20122, Milan, Italy.
** Corresponding author. Istituto Nazionale Genetica Molecolare "Romeo ed Enrica Invernizzi", 20122, Milan, Italy.
E-mail addresses: albanese@ingm.org (M. Albanese), defrancesco@ingm.org (R. De Francesco).
[1] These authors contributed equally.
[2] Lead contact.
[3] Current address: Department of Experimental Oncology, European Institute of Oncology (IEO)-IRCCS, Milan, Italy.

https://doi.org/10.1016/j.virol.2025.110659
Received 14 May 2025; Received in revised form 18 July 2025; Accepted 14 August 2025
Available online 15 August 2025

and constant evolution of SARS-CoV-2 continues to challenge the long-term efficacy of these treatments. In particular, several SARS-CoV-2 variants of concern (VOCs) have emerged, showing improved transmissibility, evasion of immunity, or changes in virulence (Telenti et al., 2022). Since vaccine development mainly targets the virus' Spike protein, the effectiveness of the vaccine against the currently predominant variant may not extend to subsequent variants (Gómez et al., 2021).

SARS-CoV-2 belongs to the Coronaviridae family, a group of positive-sense, single-stranded RNA viruses known for infecting a wide range of mammals and birds (Mingaleeva et al., 2022). Approximately two-thirds of the SARS-CoV-2 genome is occupied by two large ORFs (i.e. ORF1a and ORF1b) which encode 16 non-structural proteins (NSPs) required for viral RNA synthesis, expression and maturation (V'kovski et al., 2021). ORF1a and ORF1b encode the polyproteins pp1a and pp1ab, respectively, from which NSPs are released by proteolytic cleavage. This cleavage is carried out by two NSPs that function as cysteine proteases: NSP3, also known as papain-like protease (PLpro), is responsible for the release of NSP1-3 and the amino terminus of NSP4, while NSP5, referred to as the main protease (Mpro) or 3-chymotrypsin-like protease (3CLpro), releases NSP5-16 and the carboxy terminus of NSP4 (Xia and Kang, 2011). These two proteases, PLpro and Mpro, play an essential role in the life cycle of SARS-CoV-2, allowing the release of proteins necessary for genome replication from polyprotein precursors. The key role of these two proteases, combined with the fact that they are not subjected to the same extensive evolutionary pressure as the Spike protein, makes them highly attractive drug targets, as they exhibit minimal variability across different viral variants (Diogo et al., 2024). Mpro is responsible for the release of most non-structural proteins (NSPs), and has a more compact and less complex structure than PLpro. The most promising therapeutic applications have been developed to target both proteases (Citarella et al., 2023; Tan et al., 2024; Garnsey et al., 2024).

The first FDA-approved drug targeting SARS-CoV-2's Mpro was Nirmatrelvir, a component of the oral antiviral combination drug Paxlovid, which resulted in a reduction in the risk of severe COVID-19 progression for current variants (Wang et al., 2024; Vangeel et al., 2022). The development of specific reporter systems to detect the activity of Mpro can facilitate the development of other drugs against these important targets, and several strategies have been developed to achieve this goal (Ma et al., 2021, 2022; Rothan and Teoh, 2021; Tillmanns et al., 2024; Narayanan et al., 2022; Zhang et al., 2024).

In this work, we introduce the i-NSP4/5-Gluc-2, a rapid and user-friendly SARS-CoV-2 reporter system based on a luminescence readout sensitive to the proteolytic activity of Mpro. This system can be adopted in a viral-free setup, making it safer and more accessible for a variety of research environments. Using this reporter system, we have established a simple and effective pipeline to evaluate the activity of drugs targeting SARS-CoV-2 protease activity, potentially enabling the simultaneous testing of hundreds of compounds simultaneously. Additionally, this system is also suitable for high-throughput screening of antiviral inhibitors and can be easily adapted to accommodate emerging SARS-CoV-2 protease mutants in the future.

2. Materials and methods

2.1. Cell lines and culture

HEK293TN cells (HEK293, CRL-3216) were maintained in Dulbecco's Modified Eagle Medium (DMEM, Gibco - Life Technologies: 4.5 g/L of D-glucose, 0.11 g/L of Sodium Pyruvate) complemented with 10 % of fetal bovine serum (FBS, Gibco - LifeTechnologies), 1 % of Glutamine (L-Glutamine 100X-Euroclone), 1 % Penicillin-Streptomycin (P/S, 100X - Euroclone), 1 % sodium pyruvate (NaPyruvate, Gibco, LifeTechnologies) and 1 % non-essential amino acids (NEAA, Gibco, LifeTechnologies). HEK293TN-hACE2 cell line was generated by lentiviral transduction of HEK293TN to stably express hACE2 receptor. Lentiviral vectors were produced by co-transfection (calcium phosphate-based method) of third generation helper and transfer plasmids (see 3.4). pLENTI_hACE2_HygR transfer plasmid carrying both hACE2 receptor and hygromycin resistance (Addgene #155296) was used. 48h after transduction, HEK293TN were subjected to hygromycin selection (250 μg/mL) to isolate hACE2 expressing cells. Expression of hACE2 was confirmed by flow cytometry using anti-hACE2 antibodies. HEK293TN-hACE2 cells were maintained in the same culture conditions of HEK293TN, with the addition of 250 μg/mL Hygromycin (Gibco). HEK293TN-hACE2 were used for infection experiments with SARS-CoV-2.

2.2. I-NSP-Gluc plasmids generation

i-NSP-Gluc encoding plasmids were generated by cloning from i-TEVp-Gluc Double plasmid. First, the vector plasmid was digested with different restriction enzymes *Bam*HI-HF and *Nhe*I-HF (NEB) (with Mpro cleavage sequence into site 1), whereas *Age*I-HF and *Eco*RI-HF (NEB) (with Mpro cleavage sequence into site 2). The digested plasmids were purified from gel with Wizard SV kit (Promega). according to the kit instructions. We designed two custom oligos pairs (see Table S1) to selectively clone each of the 11 SARS-CoV-2 cleavage sequences sensitive to Mpro activity. Plasmid DNA purification from transformed bacterial suspension was carried out using NucleoBond Xtra Maxi Kit (Macherey-Nagel) following the manufacturer protocols. Final elution was performed in water. Plasmid DNA was quantified by Nanodrop. Primers annealing reaction was performed adding 1 μL of both reverse and forward primers (stock 100 μM) to 18 μL of annealing buffer (NaCl 20 mM and Tris-HCl pH8 10 mM), the solution was then put in Thermocycler (T3000, Biometra) at 95 °C. After 5 min, the temperature was reduced slowly to 25 °C in 1h. At the end of the reaction, custom oligos were annealed. Ligation reaction was performed using T4 DNA ligase (BioLabs). 50 ng of vector and 1 μL of diluted custom oligos solution were added to ligation buffer: 1 μL of T4 DNA ligase (40 U/mL) and 2 μL T4 DNA ligase buffer (BioLabs). The solution was incubated at 16 °C overnight, then transformed in One ShotTM TOP10 Chemically Competent E. coli (Invitrogen).

2.3. Transient transfection

To transfect both i-NSP-Gluc2 encoding plasmid and Mpro encoding plasmid into HEK293TN cells, a Lipofectamine 2000 (Invitrogen - LifeTechnologies) transfection was performed. First, HEK293TN cells were seeded in a 96-well plate at 10,000 cells/well density in 100 μL of DMEM medium (Invitrogen – LifeTechnologies). The following day, Lipofectamine was added to Opti-MEM (Gibco – LifeTechnologies) according to protocol and incubated for 5 min at room temperature. At the same time, 10 ng of vector plasmid and 1 ng of protease plasmid were added to Opti-MEM. The solutions are then mixed together and incubated for 20 min at room temperature before being added to HEK293TN.

2.4. Cells treatment

To evaluate antiviral activity of different compounds, cells were treated with Mpro inhibitors 1h after transfection. The compounds, dissolved in DMSO stock solution, were diluted to 3x final desired concentration in 50 μL of DMEM. The percentage of DMSO contained in each well should not exceed 1–2 % of the total volume, as DMSO is cytotoxic and could affect cell viability. The bioluminescence reduction is evaluated after 48 h post treatment.

2.5. SARS-CoV-2 Mpro inhibitors infection assay

HEK293TN-hACE were plated at 5000 cells/well in white 96-well plate in 100 μl of complete DMEM plus 2 % FBS. The day after cells

were treated with 7 doses of 5-fold serially diluted compounds (3 replicates/dose) in DMSO. Plates were transferred to BSL3 and SARS-CoV-2 virus (EPI_ISL_584051) was added at 0.1 MOI in 50 μl of volume to each well. Following this procedure the higher concentration of tested compound is 10 μM and DMSO percentage is 0.25 % for all conditions. Plates were maintained in incubators at 37 °C and 72h and inhibition effect of compounds on SARS-CoV-2 replication was evaluated by cytopathic effect with CPE assay. In detail, CellTiter-Glo® Luminescent Cell Viability Assay (promega), which provides a luminescent method to determine cell viability, was used. Obtained Relative Luminescence Unit (RLU) were normalized to infected and not infected controls in order to obtain the percentage of inhibition of cytopathic effect using the following formula: *% CPE inhibition= 100*(Test Cmpd − Avg. Virus)/(Avg. Cells − Avg. Virus),* where *Avg virus* derived from Infected + vehicle (0.25 % DMSO) wells RLU while Avg. Cells derived from Not Infected + vehicle (0.25 % DMSO) wells RLU. Dose response curve were generated by nonlinear regression curve fitting with GraphPad Prism to calculate Effective Concentration that inhibit 50 % of viral cythopatic effect (IC50). Finally, compounds cytotoxicity effect was determined in a parallel plate treated with compounds but not infected using CellTiter-Blue Cell Viability Assay (promega), which provides a fluorescent method to determine cell viability. Obtained RFU are normalized to not treated wells to define compounds cytotoxicity.

2.6. Luminescence assay

Coelenterazine (PJK Biotech, CAS 55779-48-1), the native substrate of Gluc, was dissolved in ethanol to prepare a 2.5 mM stock solution and diluted 1:500 in 1X PBS (Gibco, Life Technologies) for reaction. For the assay in a 96-well plate (Thermo Scientific, 236108), 50 μL of the diluted solution was added to 50 μL of supernatant collected from transfected cells. In the 384-well plate format (Thermo Scientific, 262360), given the longer acquisition time of the plate, a more stable version of the substrate was used. For this purpose, 40 μL of reagent Gaussia Luciferase Glow Assay Kit (Thermo Scientific, 16160) was added to 40 μL of cell supernatant. Luminescence was measured using an Infinite F200 PRO Microplate Reader, with an integration time of 1000 ms for the 96-well plate and 500 ms for the 384-well plate. Before measurement, the plate was shaken for 10 s. Relative luminescence units (RLUs) were normalized to the no-protease condition (background signal). Each condition was tested in 3 or 4 independently transfected wells, for 96 or 384 plate respectively.

2.7. Viability assays

Cell viability is assessed by CellTiter-Blue™ Cell Viability Assay (CTB, Promega, G8080). The system is based on the ability of living cells to convert a redox dye (Resazurin) into a fluorescent-end product (Resorufin). Cells are incubated with the CTB solution diluted 1:5 in medium for 1h at 37 °C. The fluorescent signal is measured using InfinitieF200 PRO Microplate Reader (TECAN) with a 560Ex/590 Em filter set. All vitality values are normalized on untreated conditions and expressed as percentage of the control (100 %).

2.8. iGluc score

The iGluc Score is a quantitative metric designed to evaluate the efficacy of drugs based on their ability to inhibit a specific biological activity while normalizing for the potential confounding effects of cell viability. It provides a comparative measure of the residual activity (RA) of a biological system, such as a viral infection or cellular pathway, under different drug concentrations. The iGluc Score facilitates the detection of dose-response relationships by comparing residual activity at low and high drug concentrations, identifying compounds with clear, concentration-dependent inhibition.

The iGluc Score is calculated as the ratio between residual activity at a high drug concentration (in this work 50 μM) and residual activity at a low drug concentration (in this work 10 μM), with both values normalized to account for cell viability.

The formula for the iGluc score is reported here:

$$iGluc\ score = \frac{RA50/log\ 10(vit50)}{RA10/log\ 10(vit10)}$$

where, Residual Activity (RA) represents the biological activity that remains in the presence of the drug at 50 μM (RA50) and at 10 μM (RA10). Vitality (vit) indicates the percentage of cells that survive at 50 μM (vit50) and 10 μM (vit10) of the analyzed compound. Normalizing each RA to the viability of the cells at that concentration ensures that the impact of cell viability is properly accounted for, preventing confounding effects from cytotoxicity. The average of the obtained iGluc Score from multiple biological replicates was then used to evaluate drug efficacy. A lower iGluc Score indicates higher efficacy, as it reflects a significant reduction in biological activity at high drug concentrations compared to low concentrations, while a higher iGluc Score suggests that the drug has limited or no inhibitory effect on the target activity, even at higher concentrations. A threshold at 0.75 was set to have a sensitive and specific evaluation of the active compounds. Sensitivity and specificity are calculated using MedCalc Software Ltd. Diagnostic test evaluation calculator. https://www.medcalc.org/calc/diagnostic_test.php.

2.9. Material availability

All materials are available upon request to defrancesco@ingm.org.

3. Results

3.1. Design of SARS-CoV-2 M^{pro} reporter system

We developed a SARS-CoV-2 Mpro-sensitive construct based on the detection of Gaussia luciferase (Gluc), building upon a system previously described by others (Bartok et al., 2013; Luft et al., 2014). Gluc was selected as the biosensor due to its natural secretion by mammalian cells, making it easily detectable through high-throughput luminescence-based assays. To retain Gluc within the cells, it was necessary to fuse it with an appropriate molecular anchor (Takenaka et al., 2008). Thus, we generated a fusion construct combining Gluc with pro-interleukin-1β (pro-IL-1β), which effectively retains Gluc in the cytoplasm. The pro-domain of interleukins has a strong tendency to form aggregates that trap Gluc within the cell, preventing interaction with its substrate and thereby inactivating it (Larionova et al., 2018).

There are two potential locations where the protease cleavage site can be inserted into the construct: site 1, which is positioned between the N-terminus and C-terminus of pro-IL-1β (corresponding to the original caspase-1 cleavage site), and site 2, which separates pro-IL-1β from Gluc (Fig. 1) (Garcia-Calvo et al., 1999).

To test the functionality of the iGluc reporter system, we introduced the Tobacco Etch Virus (TEV) protease cleavage site (TEVp) into either site 1 (single) or both sites (double) to evaluate the system's ability to detect viral protease activity. This resulted in increased Gluc activity in the supernatant as TEV protease levels rose (Supplementary Fig. 1). Interestingly, the sensitivity of the system significantly increased when the cleavage site was inserted at both locations.

Following these results, we incorporated all potential cleavage sequences recognized by Mpro into the construct. Indeed, SARS-CoV-2 Mpro recognizes 11 distinct cleavage sites located between adjacent non-structural proteins (NSPs) in the viral polyprotein. Each of these sequences was individually inserted into site 2 (Table 1), creating the i-NSP-Gluc2 construct, while site 1 retained the TEV cleavage site as a control. We then evaluated Mpro cleavage efficiency for all constructs (Fig. 2A). Notably, only the NSP4/5, NSP9/10, and NSP15/16 cleavage

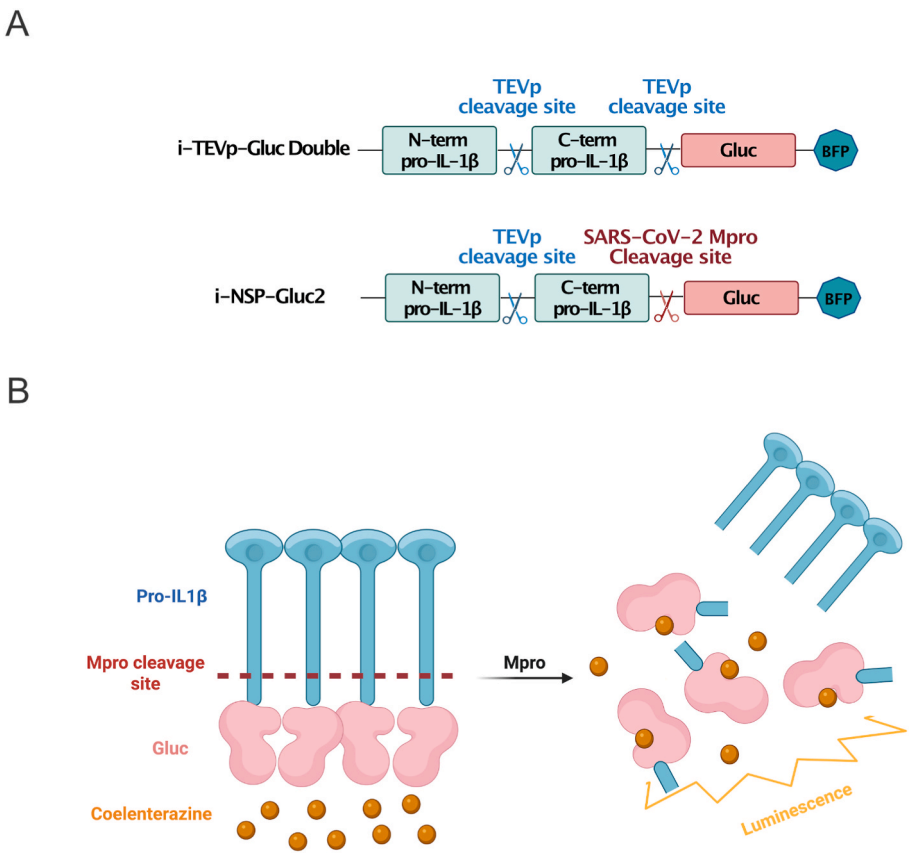

Fig. 1. iGluc activation through Mpro proteolytic cleavage. A, Schematic representation of iGluc reporter constructs. **B**, Molecular mechanism of Gluc release from pro-IL1β aggregates and its activation.

Table 1
SARS-CoV-2 cleavage sequences inserted into i-NSP-Gluc2 construct. Amino acids residues into M^{pro} cleavage sequences are identified as $P_5P_4P_3P_2P_1{\downarrow}P_1'P_2'P_3'P_4'P_5'$ position.

No.	NSP	Cleavage sequence
1	NSP 4/5	SAVLQ ↓ SGFRK
2	NSP 5/6	GVTFQ ↓ GKFKK
3	NSP 6/7	VATVQ ↓ SKMSD
4	NSP 7/8	RATLQ ↓ AIASE
5	NSP 8/9	AVKLQ ↓ NNELS
6	NSP 9/10	TVRLQ ↓ AGNAT
7	NSP 10/12	EPLMQ ↓ SADAS
8	NSP 12/13	HTVLQ ↓ AVGAC
9	NSP 13/14	VATLQ ↓ AENVT
10	NSP 14/15	FTRLQ ↓ SLENV
11	NSP 15/16	LQASQ ↓ AWQPG

sites led to a significant increase in luciferase activity in the presence of Mpro. NSP7/8 and NSP14/15 exhibited lower sensitivity while no cleavage was observed in the other constructs using our peptide-based gaussia reporter system (Fig. 2A). Among all the constructs, the NSP4/5 sequence was cleaved by Mpro with the highest efficiency, resulting in more than 9-fold increase in the signal-to-noise ratio compared to other conditions. Consequently, the i-NSP4/5-Gluc2 construct was chosen as the best candidate due to its greater sensitivity and thus selected for further experiments.

3.2. *Characterization of SARS-CoV-2 M^{pro} reporter system*

To explore whether the position of the Mpro cleavage site affects the reporter's sensitivity, we designed three constructs containing the NSP4/5 sequence at site 1, site 2, or both, named respectively i-NSP-Gluc1, i-NSP-Gluc2, i-NSP-Gluc-double (Fig. 2B) and evaluated their cleavage in the presence of Mpro activity. Contrary to our expectations, the construct with the cleavage site only at position 2 demonstrated the highest Mpro cleavage activity (Fig. 2C). As a result, the i-NSP4/5-Gluc2 construct was identified as the optimal reporter for detecting Mpro activity.

To validate the specificity of the cleavage signal observed, we employed a catalytically inactive SARS-CoV-2 Mpro mutant (C145A). C145 is one of the two critical residues forming the catalytic dyad of the protease (C145 and H41), and the C145A mutation completely abolishes Mpro activity. Co-expression of wild-type SARS-CoV-2 Mpro (WT) with i-NSP4/5-Gluc2 resulted in a significant increase in bioluminescence, whereas the inactive C145A mutant did not induce any detectable bioluminescence (Fig. 2D).

We then optimized various experimental conditions to maximize the signal-to-noise ratio, aiming to enhance the sensitivity of our reporter system to Mpro activity. To this aim, we first conducted a titration of both the Mpro-encoding plasmid and the i-NSP4/5-Gluc2-encoding plasmid (Fig. 3A and B).

From the protease titration, we observed the highest bioluminescence signal with 1–5 ng of the Mpro-encoding plasmid (Fig. 3A). Similarly, titration of the reporter plasmid showed that 12.5 ng and 6.25 ng of i-NSP4/5-Gluc2-encoding plasmid provided the highest signal-to-noise ratios (Fig. 3B). Therefore, we established the optimal experimental conditions as 1 ng of Mpro-encoding plasmid and 10 ng of i-NSP4/5-Gluc2-encoding plasmid. These conditions yielded a consistent signal-to-noise ratio of approximately 10-fold.

Finally, we compared the bioluminescence signals from the luciferase assay performed on the cell supernatant with those obtained from intracellular measurements (Fig. 3C). Gluc is naturally secreted from cells due to the presence of an N-terminal signal peptide, although non-

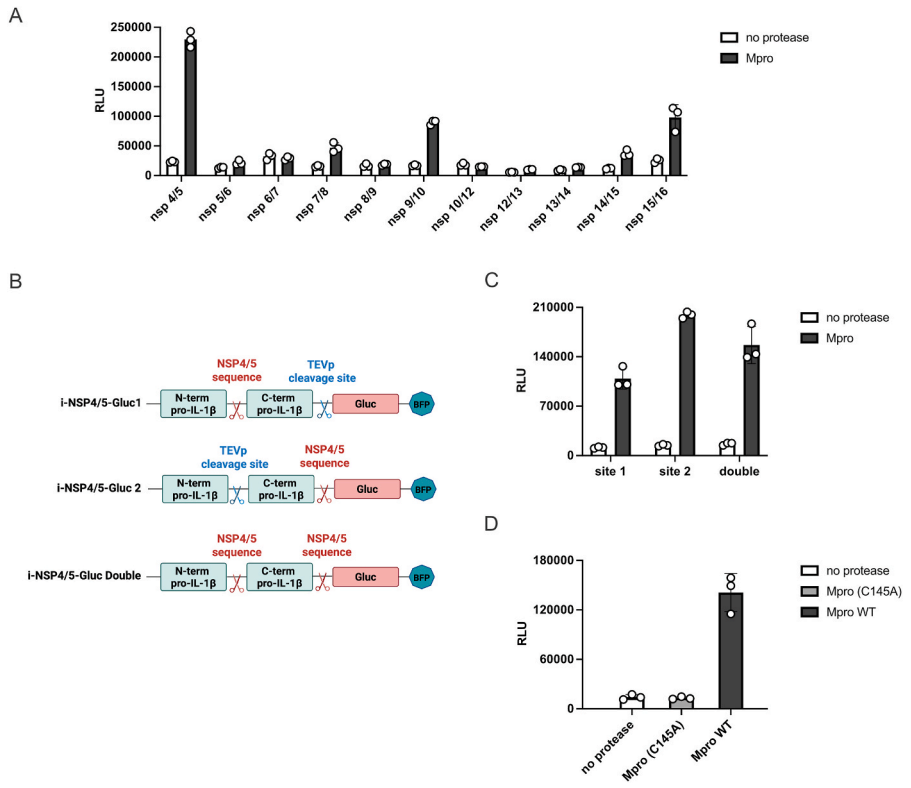

Fig. 2. Characterization of SARS-CoV-2 M^{pro} reporter system. **A**, Screening of SARS-CoV-2 sequences responsive to M^{pro} proteolytic activity, HEK-293T are co-transfected with 10 ng of IGluc containing each SARS-CoV-2 NSP sequences sensitive to Mpro and 1 ng of Mpro encoding plasmid. **B**, Schematic representation of i-NSP4/5-Gluc1, i-NSP4/5-Gluc2, and i-NSP4/5-Gluc Double. **C**, Comparison between the responsiveness of i-NSP4/5-Gluc1, -2, or -Double. **D**, Evaluation of i-NSP4/5-Gluc2 specificity co-trasfecting 1 ng of a plasmid encoding for a functional protease (Mpro WT) or an inactive mutant (Mpro C145A). Raw RLU values are shown as mean ± SD (n = 3).

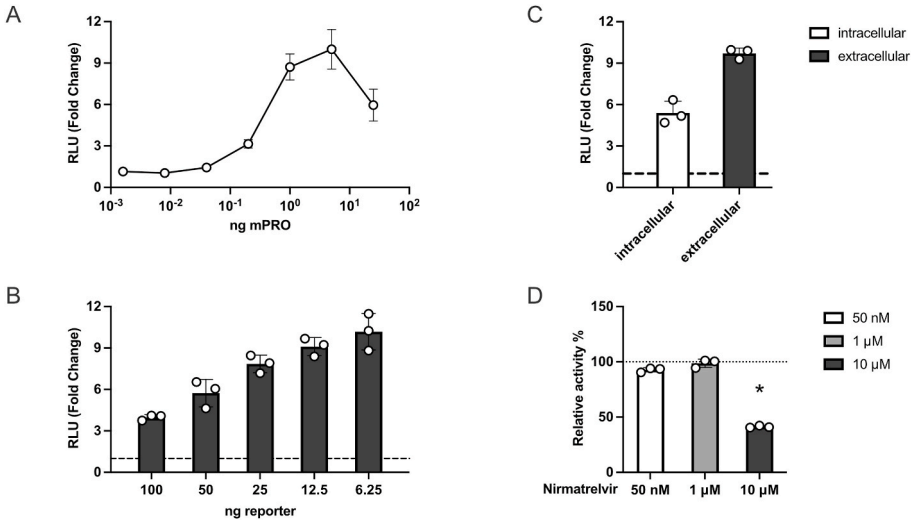

Fig. 3. i-NSP4/5-Gluc2 Experimental settings optimization. A, Optimization of Mpro concentration, Gluc signal was measured varying Mpro-encoding plasmid concentrations while keeping the i-NSP4/5-Gluc2 plasmid concentration constant at 10 ng. Normalized values against the negative control (no protease) are shown. **B**, Optimization of i-NSP4/5-Gluc2 concentration, Gluc signal was measured with varying i-NSP4/5-Gluc2 plasmid concentrations while keeping the Mpro-encoding plasmid concentration constant at 1 ng. Normalized values against the negative control (no protease) are shown **C**, Comparison between Gluc signal measured from cells supernatant (extracellular) or cell lysate (intracellular). Normalized values against the negative control (no protease) are shown **D**, Sensitivity of i-NSP4/5-Gluc2 reporter in the presence of different concentrations of Nirmatrelvir. 293T cells were transfected with 10 ng of i-NSP4/5-Gluc2 plasmid and 1 ng of Mpro-encoding plasmid. Nirmatrelvir was added at three different concentrations (50 nm, 1 μM and 50 μM) and incubated for 48 h to assess its inhibition. After that time, Gaussia luciferase activity in the supernatant was measured. The percentages of signal reduction against negative control (no treatment) are shown. Means ± SD are shown (n = 3). Statistics indicate significance by one-way ANOVA (*$p < 0.05$).

conventional secretion has been observed in the absence of this signal peptide (Tannous et al., 2005; Tannous, 2009). We sought to determine which measurement protocol produced the best assay performance between cell lysate (intracellular) and supernatant (extracellular). We found that measurement of the extracellular Gluc provided the best signal-to-noise ratio, leading us to perform all subsequent experiments using bioluminescence measurements from the cell-free supernatant having the advantage of being able to use the cells to assess their viability.

3.3. Application of the i-NSP4/5-Gluc2 reporter for drug screening

Paxlovid was the first Mpro inhibitor to receive clinical authorization from the European Medicines Agency (EMA). It consists of a combination of two drugs: Nirmatrelvir (PF07321332), which acts as a reversible covalent inhibitor of the Mpro protease, and Ritonavir. Given Nirmatrelvir's mechanism of action, we utilized it to assess whether our biosensor could effectively measure Mpro inhibition in cellular biochemical assays. At a concentration of 10 μM pf Nirmatrelvir, we could observe a reduction of Mpro activity by approximately 50.7 % (Fig. 3D).

As a proof-of-concept screen, we employed this system to evaluate the inhibitory activity of a small library of 46 candidate peptidomimetics derived from protease inhibitors (Fig. 4). Given the possible high-throughput nature of the assay, using a titration of 10 dilutions for each compound would drastically increase the number of conditions to be tested. We therefore selected only two concentrations (10 and 50 μM) for each drug that were administered 1-h post-transfection. Their inhibition of Mpro activity was assessed by measuring the reduction in luminescence signal relative to vehicle-treated controls, 48 h after treatment (Supplementary Fig. 2).

To easily quantify and visualize the inhibition of each drug in a simple but effective way we develop the iGluc Score. The iGluc score is a measure used to evaluate the efficacy of a drug. It is calculated by comparing the residual activity (RA) of the target system at high drug concentrations to the RA observed at low drug concentrations. Each RA value is normalized to account for the cell viability at the corresponding drug concentration, ensuring the score reflects a more accurate measure of the drug's effect on cellular activity independent of its toxicity (see also material and methods). Thanks to this score, we were able to identify 14 out of 46 new compounds that showed high and specific inhibition of Mpro (Fig. 4A and S2). Importantly, our positive controls, known to inhibit Mpro activity including Nirmatrelvir, Ensitrelvir, Simnotrelvir all result in iGluc scores below 1 as a result of strong and specific inhibition. Of note, this assay can be scaled down also to a 384 well format (Supplementary Fig. 3).

To prove compound efficacy in infection experiments, we performed titrations for each drug of the library and assessed their inhibition of

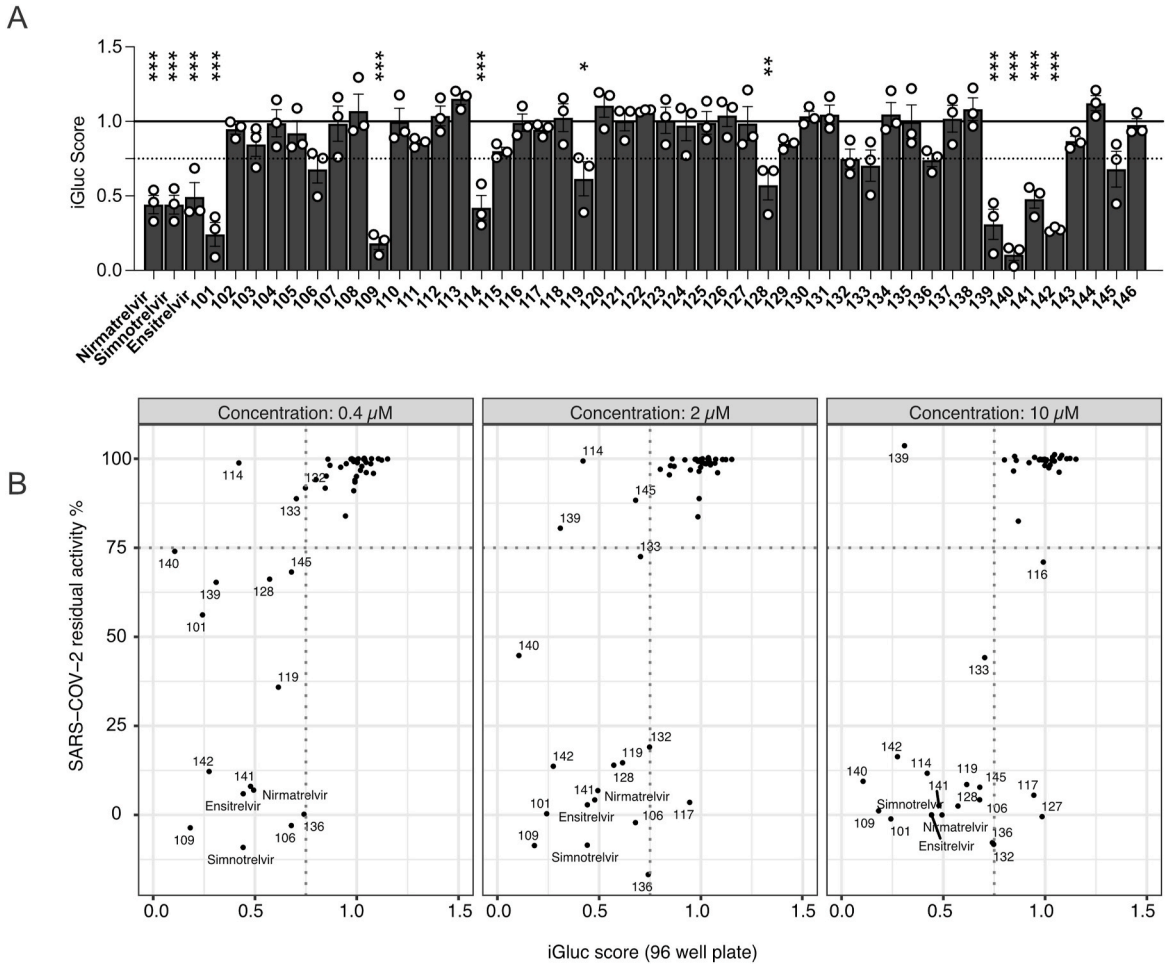

Fig. 4. iGluc Score. **A,** SARS-CoV-2 Mpro inhibitors test. Compounds were added at two different concentrations (10 and 50 μM) and incubated for 48 h to assess their inhibition. After that time, Gaussia luciferase activity in the supernatant was assessed and viability was evaluated using the cell lysate. The summary of the results was calculated using the iGluc score. Each dot represents a biological replicate. Statistics indicate significance by one-way ANOVA. (*$p < 0.05$; **$p < 0.01$; ***$p < 0.001$). **B**, Correlation between the iGluc score and inhibition of SARS-CoV-2 virus in infection experiments at different concentration values of the drugs (0.4uM, 2 μM, and 10 μM). Higher values of residual activity mean lower efficiency of the drug. Dotted lines indicate the thresholds used to consider an actual inhibition of SARS-Cov-2 (i.e. 75 % for residual activity; 0.75 for iGluc score).

SARS-CoV-2 infection in HEK293T-hACE2 cells (Supplementary Fig. 4). Our iGluc score showed a strong correlation with the inhibition observed in SARS-CoV-2 experiments at drug concentration of 0.4 μM (Spearman's rank correlation, rho = 0.71, pvalue <0.0001) and 2 μM (Spearman's rank correlation, rho = 0.66, pvalue <0.0001). A moderate correlation was also observed at 10 μM (Spearman's rank correlation, rho = 0.56, pvalue <0.0001), probably given the high concentration of drugs that have to be used during SARS-CoV-2 infection to be functional (Fig. 4B). The iGluc score demonstrated its utility in predicting functional drugs. Out of 49 drugs tested (46 of the library + 3 control drugs), only one compound selected by the iGluc score failed to significantly reduce infection (#139) (Fig. 4B), with a sensitivity of 100 % and a specificity of 88.89 % for compounds already active at 0.4 μM and with a sensitivity of 82.35 % and a specificity of 96.97 % for compounds at 10 μM. Conversely, two compounds (#117, #127) that exhibited functionality only at high concentrations in infection assays (>0.4 μM) were not identified as effective by the iGluc score (Fig. 4B and S4).

These results together validate the iGluc as a rapid, robust, and effective tool for screening and selection of active compounds among a long list of potential Mpro inhibitors, facilitating the discovery of new antiviral agents that can be easily scaled up to test hundreds of compounds simultaneously.

4. Discussion

The COVID-19 pandemic triggered an unprecedented global research effort, leading to the development of highly effective vaccines and antivirals that significantly reduced illness severity and mortality. However, the continuous evolution of SARS-CoV-2 poses challenges to the long-term effectiveness of these treatments, particularly due to emerging variants that exhibit enhanced transmissibility and immune evasion (Telenti et al., 2021; Carabelli et al., 2023).

Given the complexities of working with live SARS-CoV-2, which necessitates extensive security protocols to ensure biosafety levels, several different reporter system strategies have been developed (Rothan and Teoh, 2021; Narayanan et al., 2022; Delgado et al., 2024; Won et al., 2020; Pahmeier et al., 2021; Bei et al., 2023; Froggatt et al., 2020; Tan et al., 2023). Among the viral proteins, the main protease (Mpro) stands out due to its essential role in viral replication and its relatively conserved structure across SARS-CoV-2 variants. Unlike the spike protein, Mpro is less prone to evolutionary changes, making it an attractive target for drug development and a stable focus for reporter system strategies (Flynn et al., 2022). These systems allow researchers to safely assess Mpro activity *in vitro*, facilitating the screening of antiviral compounds without the need for live virus, thus accelerating the discovery of new therapeutics (Ren et al., 2016).

In this study, we present a luciferase-based assay designed to detect the activity of the SARS-CoV-2 Mpro protease with high scalability, simplicity, and rapid readout. To achieve this, we adapted the iGluc construct, originally developed by Bartok et al. (2013), for the assessment of Mpro activity, resulting in the creation of the i-NSP4/5-Gluc2 reporter system, which senses the presence of Mpro to produce a luminescent signal released in the cell's supernatant.

SARS-CoV-2 Mpro recognizes 11 distinct cleavage sites between adjacent non-structural proteins (NSPs). To evaluate Mpro activity on various cleavage sequences, we cloned each of the 11 Mpro-sensitive sequences into site 2 of the i-Gluc construct (i-NSP-Gluc2) (Fig. 1A and Table 1). Our findings revealed that the SAVLQ-↓-SGFRK motif, located between NSP4 and NSP5 (NSP4/5 sequence), was the most sensitive to Mpro proteolytic activity using our system (fold change up to 9.8 versus no protease control) (Fig. 2A). In contrast, the NSP9/10 and NSP15/16 sequences allowed for detection of activity but demonstrated lower sensitivity (with fold changes of 5.3 and 3.8 times respectively). This finding aligns with previous analyses using a GFP localization-based system, which indicated that the NSP15/16 site was the most sensitive, followed by NSP3/4 and then NSP4/5 and NSP9/10 (Pahmeier et al., 2021). After optimizing the experimental conditions, we demonstrated that the i-NSP4/5-Gluc2 reporter system is responsive to treatment with Nirmatrelvir, a known SARS-CoV-2 Mpro inhibitor (Fig. 3D). This system shows great promise as a rapid tool for identifying effective antivirals against SARS-CoV-2 infection. Given the highly infectious nature of SARS-CoV-2, experimental assays typically require Biosafety Level 3 (BSL3) laboratories, which significantly restrict scientific research. The i-NSP4/5-Gluc2 reporter system allows antiviral assays to be performed in BSL2 environments, thereby facilitating access to high-throughput automated handling systems and enabling the testing of a larger number of drugs and conditions (Kaufer et al., 2020).

Since the emergence of the SARS-CoV-2 pandemic, Mpro reporter assays have attracted considerable interest, resulting in the creation of various versions, many of which employ fluorescent GFP technology (Pahmeier et al., 2021; Bei et al., 2023; Froggatt et al., 2020; Tan et al., 2023). Each developed strategy presents unique advantages and disadvantages based on the molecular mechanisms underlying the constructs used but most of them are not suitable for high-throughput applications. In contrast, the i-NSP4/5-Gluc2 system utilizes a Gaussia luciferase biosensor for luminescent readouts, which offers several advantages over fluorescence or absorbance techniques. Luminescence typically provides a wider dynamic range and greater sensitivity due to lower background interference from auto-luminescence produced by compounds, media, and cells (Yang et al., 2022). Moreover, luminescence emissions can be detected with a luminescence microplate reader, enabling fast acquisition time. Gluc is naturally secreted by mammalian cells, and secreted reporters have advantages over conventional methods for monitoring gene expression: they can be quantified directly in cell-free supernatants, eliminating the need for cell lysis and preserving cells for additional analyses, such as viability assays (Supplementary Fig. 2B) (Galaway and Wright, 2020).

On top of that, other published assays rely on the use of titrated drugs with at least 8 different dilutions for each compound to be tested to have a reliable evaluation of the drug activity. Here, we introduce the iGluc Score. Thanks to this scoring algorithm, we provide a reliable yet simple value (>0.75 not functional, <0.75 functional) to assess if a compound is active or not using only 2 drug concentrations. Our pipeline using the iGluc score therefore allows us to drastically increase the number of compounds tested in a single round. Furthermore, we demonstrated that the assay can be also scaled down to a 384-well plate to have a higher throughput-friendly format (Supplementary Fig. 3). Of note, given the longer time of acquisition of the luminescent signal from a 96 well to a 384 well plate (about 4 times longer) we suggest using a more stable version of the Gaussia luciferase substrate for this specific purpose (See material and methods).

However, the i-NSP4/5-Gluc2 reporter system also has some limitations. The effective drug concentration required differs significantly from the IC50 values calculated during infection, often being an order of magnitude higher than those derived from authentic virus studies (Supplementary Fig. 4). The discrepancy stems from the i-NSP4/5-Gluc2 system's dependence on plasmid-expressed Mpro, whose levels are likely higher than those found during an infection. Since our reporter system does not account for inhibition of protease production, Mpro can accumulate. This accumulation could lead to a constant replenishment of Mpro, possibly saturating the treatment and causing us to underestimate the inhibitors' true potency. On top, the substrate of Mpro are complex viral polyproteins, and not single peptides, which might influence Mpro activity as well as drug binding and resistance (Lewandowski et al., 2025).

For these reasons, it is important to validate the hits identified by the Gaussia luciferase using a live SARS-CoV-2 infection using the Mpro within the more complex viral polyprotein.

Despite these limitations, the strong correlation between compounds identified by the score and those exhibiting functional activity in infection further supports its reliability. The iGluc score allows us to effectively distinguish between active and inactive compounds with

significantly higher sensitivity compared to similar reporter systems (Vlachou et al., 2024) with a sensitivity between 82.35 and 100 % and a specificity of 88.89–96.97 % for compounds active at 0.4 μM and 10 μM, respectively.

This approach provides a valuable pre-screening tool, significantly reducing the number of drugs requiring BSL3 infection experiments, which remain necessary to precisely calculate the IC50 of each compound (Fig. 4B). Finally, a major advantage of this reporter system is its engineering simplicity. The i-NSP4/5-Gluc2 system can easily be adapted for evaluating other proteases, not just viral ones, provided that the cleavage sequence is known (Zhang et al., 2017). By replacing the Mpro cleavage sequence in the reporter plasmid with the specific sequence for the protease of interest, and having a plasmid encoding the target protease, specific reporter systems can be developed for SARS-CoV-2 variants of concern (VOCs) or other viruses. This adaptability allows for assessments of differences in proteolytic activity or treatment responses among different proteases.

In summary, the i-NSP4/5-Gluc2 reporter system represents a significant advancement in SARS-CoV-2 drug discovery. This innovative methodology facilitates rapid and efficient screening of compound libraries offering enhanced sensitivity and specificity. By streamlining the identification of potential inhibitors, it has the potential to accelerate the development of antiviral therapeutics for COVID-19 and related coronaviruses.

CRediT authorship contribution statement

Alessandro Lucini Paioni: Writing – original draft, Visualization, Methodology, Investigation, Formal analysis, Data curation. **Lorena Donnici:** Writing – original draft, Visualization, Supervision, Methodology, Investigation, Data curation, Conceptualization. **Riccardo Nodari:** Writing – original draft, Validation. **Marika Longo Minnolo:** Methodology. **Anastasia Ferraro:** Resources. **Alessia Alberico:** Resources. **Margherita Brindisi:** Resources. **Ernesto Mejías Pérez:** Conceptualization. **Oliver T. Keppler:** Conceptualization. **Vincenzo Summa:** Resources. **Luca G. Guidotti:** Validation. **Manuel Albanese:** Writing – review & editing, Writing – original draft, Visualization, Methodology, Data curation, Conceptualization. **Raffaele De Francesco:** Writing – original draft, Validation, Supervision, Funding acquisition, Conceptualization.

Declaration of interest

The authors declare no competing interest.

Fundings

This research was supported by EU funding within the NextGenerationEU-MUR PNRR Extended Partnership initiative on Emerging Infectious Diseases (Project no. PE00000007, INF-ACT) (RN and RDF), by Piano di Sostegno alla Ricerca 2024 - Linea 2 (RN), and by the my first seed Grant-SARSVoCsCoFact UNIMI (MA).

Declaration of competing interest

The authors declare that they have no known competing financial interests or personal relationships that could have appeared to influence the work reported in this paper.

Glossary

VOC	Variant of concern
Mpro	main viral protease
3CL	pro 3C-like protease
SARS-CoV-2	Severe acute respiratory syndrome coronavirus 2
Gluc	Gaussia luciferase
iGluc	inducible Gaussia luciferase
BSL	Biosafety Level
COVID-19	Coronavirus disease 2019
ORFs	open reading frames
NSPs	non-structural proteins
PLpro	papain-like protease
TEV	Tobacco Etch Virus
TEVp	protease cleavage site
pro-IL-1β	pro-interleukin-1β
IC50	inhibitory concentration at 50 %

Appendix A. Supplementary data

Supplementary data to this article can be found online at https://doi.org/10.1016/j.virol.2025.110659.

Data availability

Data will be made available on request.

References

Bartok, E., Bauernfeind, F., Khaminets, M.G., Jakobs, C., Monks, B., Fitzgerald, K.A., Latz, E., Hornung, V., 2013. IGLuc: a luciferase-based inflammasome and protease activity reporter. Nat. Methods 10, 147–154. https://doi.org/10.1038/nmeth.2327.

Bei, Z.C., Yu, H., Wang, H., Li, Q., Wang, B., Zhang, D., Xu, L., Zhao, L., Dong, S., Song, Y., 2023. Orthogonal dual reporter-based gain-of-signal assay for probing SARS-CoV-2 3CL protease activity in living cells: inhibitor identification and mutation investigation. Emerg Microbes Infect 12. https://doi.org/10.1080/22221751.2023.2211688.

Carabelli, A.M., Peacock, T.P., Thorne, L.G., Harvey, W.T., Hughes, J., de Silva, T.I., Peacock, S.J., Barclay, W.S., de Silva, T.I., Towers, G.J., et al., 2023. SARS-CoV-2 variant biology: immune escape, transmission and fitness. Nat. Rev. Microbiol. 21, 162–177. https://doi.org/10.1038/s41579-022-00841-7.

Citarella, A., Dimasi, A., Moi, D., Passarella, D., Scala, A., Piperno, A., Micale, N., 2023. Recent advances in SARS-CoV-2 main protease inhibitors: from Nirmatrelvir to future perspectives. Biomolecules 13. https://doi.org/10.3390/biom13091339.

Delgado, R., Vishwakarma, J., Moghadasi, S.A., Otsuka, Y., Shumate, J., Cuell, A., Tansiongco, M., Cooley, C.B., Chen, Y., Dabrowska, A., et al., 2024. SARS-CoV-2 mpro inhibitor identification using a cellular gain-of-signal assay for high-throughput screening. SLAS Discovery 29. https://doi.org/10.1016/j.slasd.2024.100181.

Diogo, M.A., Cabral, A.G.T., de Oliveira, R.B., 2024. Advances in the search for SARS-CoV-2 mpro and PLpro inhibitors. Pathogens 13. https://doi.org/10.3390/pathogens13100825.

Flynn, J.M., Samant, N., Schneider-Nachum, G., Barkan, D.T., Yilmaz, N.K., Schiffer, C.A., Moquin, S.A., Dovala, D., Bolon, D.N.A., 2022. Comprehensive fitness landscape of SARS-CoV-2 Mpro reveals insights into viral resistance mechanisms. eLife 11, 1–27. https://doi.org/10.7554/eLife.77433.

Froggatt, H.M., Heaton, B.E., Heaton, N.S., 2020. Development of a fluorescence-based, high-throughput SARS-CoV-2 3CL pro reporter Assay. J. Virol. 94, 1–9. https://doi.org/10.1128/jvi.01265-20.

Galaway, F., Wright, G.J., 2020. Rapid and sensitive large-scale screening of low affinity extracellular receptor protein interactions by using reaction induced inhibition of Gaussia Luciferase. Sci. Rep. 10, 1–9. https://doi.org/10.1038/s41598-020-67468-7.

Garcia-Calvo, M., Peterson, E.P., Rasper, D.M., Vaillancourt, J.P., Zamboni, R., Nicholson, D.W., Thornberry, N.A., 1999. Purification and catalytic properties of human caspase family members. Cell Death Differ. 6, 362–369. https://doi.org/10.1038/sj.cdd.4400497.

Garnsey, M.R., Robinson, M.C., Nguyen, L.T., Cardin, R., Tillotson, J., Mashalidis, E., Yu, A., Aschenbrenner, L., Balesano, A., Behzadi, A., et al., 2024. Discovery of SARS-CoV-2 papain-like protease (PLpro) inhibitors with efficacy in a murine infection model. Sci. Adv. 10, 1–10. https://doi.org/10.1126/sciadv.ado4288.

Gómez, C.E., Perdiguero, B., Esteban, M., 2021. Emerging Sars-Cov-2 variants and impact in global vaccination programs against Sars-Cov-2/Covid-19. Vaccines (Basel) 9, 1–13. https://doi.org/10.3390/vaccines9030243.

Kaufer, A.M., Theis, T., Lau, K.A., Gray, J.L., Rawlinson, W.D., 2020. Laboratory biosafety measures involving SARS-CoV-2 and the classification as a risk group 3 biological agent. Pathology 52, 790–795. https://doi.org/10.1016/j.pathol.2020.09.006.

Larionova, M.D., Markova, S.V., Vysotski, E.S., 2018. Bioluminescent and structural features of native folded Gaussia luciferase. J. Photochem. Photobiol., B 183, 309–317. https://doi.org/10.1016/j.jphotobiol.2018.04.050.

Lewandowski, E.M., Zhang, X., Tan, H., Jaskolka-Brown, A., Kohaal, N., Frazier, A., Madsen, J.J., Jacobs, L.M.C., Wang, J., Chen, Y., 2025. Distal protein-protein interactions contribute to Nirmatrelvir resistance. Nat. Commun. 16, 1–8. https://doi.org/10.1038/s41467-025-56651-x.

Luft, C., Freeman, J., Elliott, D., Al-Tamimi, N., Kriston-Vizi, J., Heintze, J., Lindenschmidt, I., Seed, B., Ketteler, R., 2014. Application of Gaussia luciferase in

bicistronic and non-conventional secretion reporter constructs. BMC Biochem. 15, 1–12. https://doi.org/10.1186/1471-2091-15-14.
Ma, C., Xia, Z., Sacco, M.C., Hu, Y., Townsend, J.A., Meng, X., Choza, J., Tan, H., Jang, J., Gongora, M.V., Zhang, X., Zhang, F., Xiang, Y., Marty, M.T., Chen, Y., Wang, J., 2021. Discovery of Di- and trihaloacetamides as covalent SARS-CoV-2 main protease inhibitors with high target specificity. J. Am. Chem. Soc. 143 (49), 20697–20709. https://doi.org/10.1021/jacs.1c08060.
Ma, C., Tan, H., Choza, J., Wang, Y., Wang, J., 2022. Validation and invalidation of SARS-CoV-2 main protease inhibitors using the Flip-GFP and protease-glo luciferase assays. Acta Pharm. Sin. B 12, 1636–1651. https://doi.org/10.1016/j.apsb.2021.10.026.
Mingaleeva, R.N., Nigmatulina, N.A., Sharafetdinova, L.M., Romozanova, A.M., Gabdoulkhakova, A.G., Filina, Y.V., Shavaliyev, R.F., Rizvanov, A.A., Miftakhova, R. R., 2022. Biology of the SARS-CoV-2 coronavirus. Biochemistry (Mosc.) 87, 1662–1678. https://doi.org/10.1134/S0006297922120215.
Narayanan, A., Narwal, M., Majowicz, S.A., Varricchio, C., Toner, S.A., Ballatore, C., Brancale, A., Murakami, K.S., Jose, J., 2022. Identification of SARS-CoV-2 inhibitors targeting Mpro and PLpro using in-cell-protease assay. Commun. Biol. 5, 1–17. https://doi.org/10.1038/s42003-022-03090-9.
Pahmeier, F., Neufeldt, C.J., Cerikan, B., Prasad, V., Pape, C., Laketa, V., Ruggieri, A., Bartenschlager, R., Cortese, M., 2021. A versatile reporter system to monitor virus-infected cells and its application to Dengue virus and SARS-CoV-2. J. Virol. 95. https://doi.org/10.1128/jvi.01715-20.
Patel, R., Kaki, M., Potluri, V.S., Kahar, P., Khanna, D., 2022. A comprehensive review of SARS-CoV-2 vaccines: Pfizer, moderna & Johnson & Johnson. Hum Vaccin Immunother 18, 1–12. https://doi.org/10.1080/21645515.2021.2002083.
Ren, L., Peng, Z., Chen, X., Ouyang, H., 2016. Live cell reporter systems for positive-sense single strand RNA viruses. Appl. Biochem. Biotechnol. 178, 1567–1585. https://doi.org/10.1007/s12010-015-1968-5.
Rothan, H.A., Teoh, T.C., 2021. Cell-based high-throughput screening protocol for discovering antiviral inhibitors against SARS-COV-2 main protease (3CLpro). Mol. Biotechnol. 63, 240–248. https://doi.org/10.1007/s12033-021-00299-7.
Takenaka, Y., Masuda, H., Yamaguchi, A., Nishikawa, S., Shigeri, Y., Yoshida, Y., Mizuno, H., 2008. Two forms of secreted and thermostable luciferases from the Marine copepod Crustacean, Metridia Pacifica. Gene 425, 28–35. https://doi.org/10.1016/j.gene.2008.07.041.
Tan, H., Hu, Y., Wang, J., 2023. FlipGFP protease assay for evaluating in vitro inhibitory activity against SARS-CoV-2 Mpro and PLpro. STAR Protoc 4. https://doi.org/10.1016/j.xpro.2023.102323.
Tan, B., Zhang, X., Ansari, A., Jadhav, P., Tan, H., Li, K., Chopra, A., Ford, A., Chi, X., Ruiz, F.X., et al., 2024. Design of a SARS-CoV-2 papain-like protease inhibitor with antiviral efficacy in a mouse model. Science 383, 1434–1440. https://doi.org/10.1126/science.adm9724, 1979.
Tannous, B.A., 2009. Gaussia luciferase reporter assay for monitoring biological processes in culture and in vivo. Nat. Protoc. 4, 582–591. https://doi.org/10.1038/nprot.2009.28.
Tannous, B.A., Kim, D.E., Fernandez, J.L., Weissleder, R., Breakefield, X.O., 2005. Codon-optimized Gaussia luciferase CDNA for Mammalian gene expression in culture and in vivo. Mol. Ther. 11, 435–443. https://doi.org/10.1016/j.ymthe.2004.10.016.
Telenti, A., Arvin, A., Corey, L., Corti, D., Diamond, M.S., García-Sastre, A., Garry, R.F., Holmes, E.C., Pang, P.S., Virgin, H.W., 2021. After the pandemic: perspectives on the future trajectory of COVID-19. Nature 596, 495–504. https://doi.org/10.1038/s41586-021-03792-w.
Telenti, A., Hodcroft, E.B., Robertson, D.L., 2022. The evolution and biology of SARS-CoV-2 variants. Cold Spring Harb. Perspect. Med. 12. https://doi.org/10.1101/cshperspect.a041390.
Tillmanns, J., Kicuntod, J., Ehring, A., Elbasani, E., Borst, E.M., Obergfäll, D., Müller, R., Hahn, F., Marschall, M., 2024. Establishment of a luciferase-based reporter system to study aspects of human Cytomegalovirus infection, replication characteristics, and antiviral drug efficacy. Pathogens 13. https://doi.org/10.3390/pathogens13080645.
Vangeel, L., Chiu, W., De Jonghe, S., Maes, P., Slechten, B., Raymenants, J., André, E., Leyssen, P., Neyts, J., Jochmans, D. Remdesivir, 2022. Molnupiravir and Nirmatrelvir remain active against SARS-CoV-2 omicron and other variants of concern. Antiviral Res 198, 10–12. https://doi.org/10.1016/j.antiviral.2022.105252.
Vlachou, A., Nchioua, R., Regensburger, K., Kirchhoff, F., Kmiec, D., 2024. A Gaussia luciferase reporter assay for the evaluation of Coronavirus Nsp5/3CLpro activity. Sci. Rep. 14, 1–13. https://doi.org/10.1038/s41598-024-71305-6.
V'kovski, P., Kratzel, A., Steiner, S., Stalder, H., Thiel, V., 2021. Coronavirus biology and replication: implications for SARS-CoV-2. Nat. Rev. Microbiol. 19, 155–170.
Wang, L., Ding, Z., Wang, Z., Zhao, Y., Wu, H., Wei, Q., Gao, L., Han, J., 2024. The development of an oral solution containing Nirmatrelvir and ritonavir and assessment of its pharmacokinetics and stability. Pharmaceutics 16. https://doi.org/10.3390/pharmaceutics16010109.
Won, J., Lee, S., Park, M., Kim, T.Y., Park, M.G., Choi, B.Y., Kim, D., Chang, H., Heo, W. Do, Kim, V.N., et al., 2020. Erratum: development of a laboratory-safe and low-cost detection protocol for SARS-CoV-2 of the coronavirus disease 2019 (COVID-19). (Experimental Neurobiology 29 (2), 107–119. https://doi.org/10.5607/En.20009. Exp Neurobiol 2020, 29, 402, doi:10.5607/EN20009E1.
Xia, B., Kang, X., 2011. Activation and maturation of SARS-CoV main protease. Protein Cell 2, 282–290. https://doi.org/10.1007/s13238-011-1034-1.
Yang, M., Zeng, Z., Lam, J.W.Y., Fan, J., Pu, K., Tang, B.Z., 2022. State-of-the-Art self-luminescence: a win-win situation. Chem. Soc. Rev. 51, 8815–8831. https://doi.org/10.1039/d2cs00228k.
Zhang, Y., Ke, X., Zheng, C., Liu, Y., Xie, L., Zheng, Z., Wang, H., 2017. Development of a luciferase-based biosensor to assess enterovirus 71 3C protease activity in living cells. Sci. Rep. 7. https://doi.org/10.1038/s41598-017-10840-x.
Zhang, R., Yan, H., Zhou, J., Yan, G., Liu, X., Shang, C., Chen, Y., 2024. Improved fluorescence-based assay for rapid screening and evaluation of SARS-CoV-2 main protease inhibitors. J. Med. Virol. 96. https://doi.org/10.1002/jmv.29498.